Astron. Astrophys. 330, 549–558 (1998)

ASTRONOMY AND ASTROPHYSICS

Millimeter continuum observations of X-ray selected T Tauri stars in Ophiuchus⋆

Dieter Nürnberger[1], **Wolfgang Brandner**[1,2], **Harold W. Yorke**[1], **and Hans Zinnecker**[3]

[1] Astronomisches Institut der Universität Würzburg, Am Hubland, D-97074 Würzburg, Germany
(nurnberg@astro.uni-wuerzburg.de), (brandner@astro.uni-wuerzburg.de), (yorke@astro.uni-wuerzburg.de)
[2] Department of Astronomy, University of Illinois at Urbana-Champaign, 1002 West Green Street, Urbana, IL 61801, USA
(brandner@astro.uiuc.edu)
[3] Astrophysikalisches Institut Potsdam, An der Sternwarte 16, D-14482 Potsdam, Germany (hzinnecker@aip.de)

Received 13 March 1997 / Accepted 22 September 1997

Abstract. We present the results of 1.3 mm dust continuum observations for a sample of 17 X-ray selected T Tauri stars in the Ophiuchus star forming region performed with the MPIfR 7-channel bolometer array mounted at the IRAM 30 m Millimeter Radio Telescope. We have detected cold dust emission from 3 of the objects and have derived 3σ upper limits (~ 21 mJy on average) for the remaining objects. These upper limits suggest that the disk masses (gas + dust) are less than $5 \cdot 10^{-3}\,M_\odot$.

Combining our results with those obtained by André & Montmerle (1994) for a sample of 21 X-ray selected T Tauri stars (3 additional detections) we improve the statistical significance of our conclusions. As the frequency of circumstellar disks and the disk properties might depend on the selection criteria as well as local conditions, comparison is made with 1.3 mm surveys of Hα selected T Tauri stars in Chamaeleon, Lupus, Ophiuchus, and Taurus-Auriga.

In order to study the mass of cold dust in multiple systems we also observed a sample of 15 well known binaries, triples, and quadruples by 1.3 mm photometry. From these observations we report the 1.3 mm detection of 4 multiple systems. It seems that the measured 1.3 mm flux density increases slightly with increasing binary separation.

In addition, we have mapped the hierarchical triple SR 24 at $\lambda = 1.3$ mm with the 7-channel bolometer array. We detected cold dust emission only from the southern component with a peak intensity of ~ 230 mJy and a corresponding circumstellar disk mass of $\sim 0.035\,M_\odot$ (gas + dust), while for the northern component we derived an upper limit of 10 % of the SR 24S peak flux density. The non-detection of 1.3 mm emission from SR 24N suggests a lack of cold circumstellar dust in the outer part of the disk, which might have been cleared by the close infrared companion $0\farcs2$ away from SR 24N.

Key words: stars: circumstellar matter – stars: formation – stars: late-type – stars: low-mass – stars: pre-main sequence – radio continuum: stars

1. Introduction

The evolutionary classification scheme of young stellar objects (YSOs) originally introduced by Lada (1987) and subsequently revised and extended by André & Montmerle (1994) is based on the infrared (IR) excess of the sources, as measured by the spectral index $\alpha_{\rm IR} = {\rm d}\log(\lambda F_\lambda)\,/\,{\rm d}\log\lambda$ between $\lambda = 2.2$ and 10 μm. As this excess is attributed to the presence of circumstellar dust, the IR classification predicts a progressive decrease of the amount of circumstellar material from IR class 0 to IR class III, i.e. a decrease with stellar age. For embedded sources (IR class 0 / I; $\alpha_{\rm IR} > 0$) most of the circumstellar matter is distributed in a extended infalling envelope with a typical size of about 10^4 AU (e.g. Adams et al. 1987, Terebey et al. 1993), while for the later stages of T Tauri stars (IR class II / III; $\alpha_{\rm IR} < 0$) the IR emission arises from circumstellar disks on the order of 100 AU in size (e.g. Adams et al. 1988, Bertout et al. 1988, André & Montmerle 1994). However, there is some ambiguity in this classification scheme. Depending on the orientation of its circumstellar accretion disk a class II / III source could mimic the spectral characteristics of a class I source (Yorke et al. 1995, Sonnhalter et al. 1995).

In any case, infrared observations give only poor estimates of the amount of circumstellar material around YSOs, as shortward of 100 μm massive envelopes / disks are generally optically thick. Furthermore, the IR range is also rather sensitive to the temperature and density distribution of the circumstellar material and probes only the warm regions close to the central star. On the other hand, dusty envelopes / disks around pre-main sequence (PMS) stars are optically thin at wavelengths of the

Send offprint requests to: Dieter Nürnberger

⋆ Based on observations obtained with the IRAM 30 m MRT on Pico Veleta, Spain

order of 1 mm. Thus, observations of dust continuum emission in the mm range provide a better tool to trace the circumstellar evolution of YSOs (e.g. Beckwith et al. 1990, André & Montmerle 1994) than infrared observations.

Traditionally, T Tauri stars are found in either Hα emission line surveys (both classical and weak-line T Tauri stars; CTTS and WTTS, respectively) or because of their X-ray emission (mostly WTTS). In recent years several 1.3 mm surveys have been conducted (e.g. Beckwith et al. 1990, Henning et al. 1993, Osterloh & Beckwith 1995, André & Montmerle 1994, Nürnberger et al. 1997) which have addressed the question of dust continuum emission of Hα selected T Tauri stars. Only in a few cases (e.g. André & Montmerle 1994) X-ray selected T Tauri stars were also taken into consideration.

In order to examine whether there is a relationship between X-ray activity and the presence of (cool) circumstellar material, we here present a study of the millimeter properties of an X-ray flux limited sample of T Tauri stars, which have been detected with the Einstein Observatory by Montmerle et al. (1983). Typical X-ray luminosities of $L_X = (0.5 \ldots 25) \cdot 10^{30}$ erg s^{-1} and large variations of the X-ray fluxes due to strong stellar flares (e.g. Preibisch et al. 1993) are indicative of the T Tauri nature of these stars. Estimates of temperature and density of the X-ray emitting plasma, timescales of the X-ray variability, and distribution of the X-ray luminosities (see e.g. review by Montmerle & Casanova 1995) indicate that the X-ray emission originates from magnetically active stars. This activity is solar-like and might be due to a dynamo mechanism associated with convective motions (cf. discussion in Feigelson et al. 1993, Montmerle et al. 1994).

Most of the X-ray sources investigated here are distributed at the periphery ($A_V < 10^m$) of the densest regions of the ρ Ophiuchi molecular cloud. Thus, our sample of sources is distinguished both from those of spatially widely distributed WTTS detected by ROSAT (e.g. Alcalá et al. 1995, Neuhäuser et al. 1995, Sterzik et al. 1995, Wichmann et al. 1996, 1997) and X-ray sources embedded in dense cloud cores (Casanova et al. 1995).

2. Observations and data reduction

The observations were performed in March 1993 at the IRAM 30 m Millimeter Radio Telescope (MRT; Baars et al. 1987) equipped with the MPIfR 7-channel bolometer array (Kreysa 1992). The half power beam width (HPBW) of the telescope was $\sim 12''$. Chopping was done with the focal plane chopper operating with a beam separation of $30''$ in azimuth. The quality of the telescope pointing was estimated to be about $3''$, while the stellar coordinates were taken from Bouvier & Appenzeller (1992) and are accurate within $\pm 2''$.

Both the 17 ρ Ophiuchi X-ray selected (ROX) sources and 15 multiple systems were studied by 1.3 mm photometry with the 7-channel bolometer array, which performed ON-OFF measurements consisting of 10 cycles with 20 s integration time each. Strong sources were observed at least twice, fainter objects up to four times. For each scan a baseline calculated from the six outer

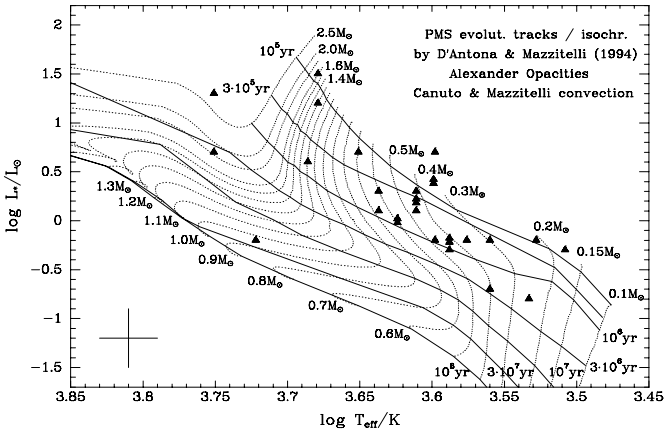

Fig. 1. H-R diagram of the sample of 38 X-ray selected T Tauri stars in Ophiuchus. The PMS evolutionary tracks and isochrones are taken from D'Antona & Mazzitelli (1994). The cross in the lower left corner gives log T_{eff} and log L_* errorbars typical for T Tauri stars with stellar masses of approximately 0.5 $M_\odot$ and ages of about 1 Myr.

channels of the array was subtracted from the measured flux density resulting in an overall sensitivity of about 21 mJy beam^{-1} (3σ). The atmospheric opacity frequently determined by skydips was relatively unstable with daily average values between 0.4 and 0.5 at zenith. Uranus was used as calibration standard adopting a brightness temperature of 95 K at 1.3 mm and an estimated absolute calibration uncertainty of ± 20 % (Thum et al. 1992). IRAS 16293-2422, a well-known class 0 source and strong mm emitter ($F_{1.3mm} = 5186 \pm 195$ mJy; see also measurements by Mezger et al. 1992, Walker et al. 1993, André & Montmerle 1994), was observed as a secondary calibrator.

Finally, the triple system SR 24 was mapped at $\lambda = 1.3$ mm with the 7-channel bolometer array. The map data were baseline-subtracted, calibrated, and restored to 'single-beam' maps as well as converted into RA-DEC maps within the NOD2 software package. For deconvolution with a Gaussian maximum likelihood algorithm, maps of Uranus and Mars (in March 1993 their angular diameters were about $3\farcs5$ and $4\farcs0$, respectively) were used as point spread functions. The recursive deconvolution algorithm was developed by Meinel (1986) and Blecha & Richard (1989). Brandner (1992) implemented it into an IDL routine. The 3σ value obtained from the 1.3 mm photometry of SR 24 was set as boundary condition, i.e. the iterative algorithm was stopped when the average diameter of the area surrounded by the 3σ contour line was smaller than the HPBW. This criterion proved to be reliable as the algorithm's result diverges only a few iteration steps later.

3. Sample of objects

For most of the Einstein detected X-ray sources counterparts at optical and near IR wavelengths are reported by Wilking et al. (1987) and Wilking et al. (1989). Some of them even have several possible counterparts within the Einstein IPC error circle; in Table 1 these candidates are denoted by an additional

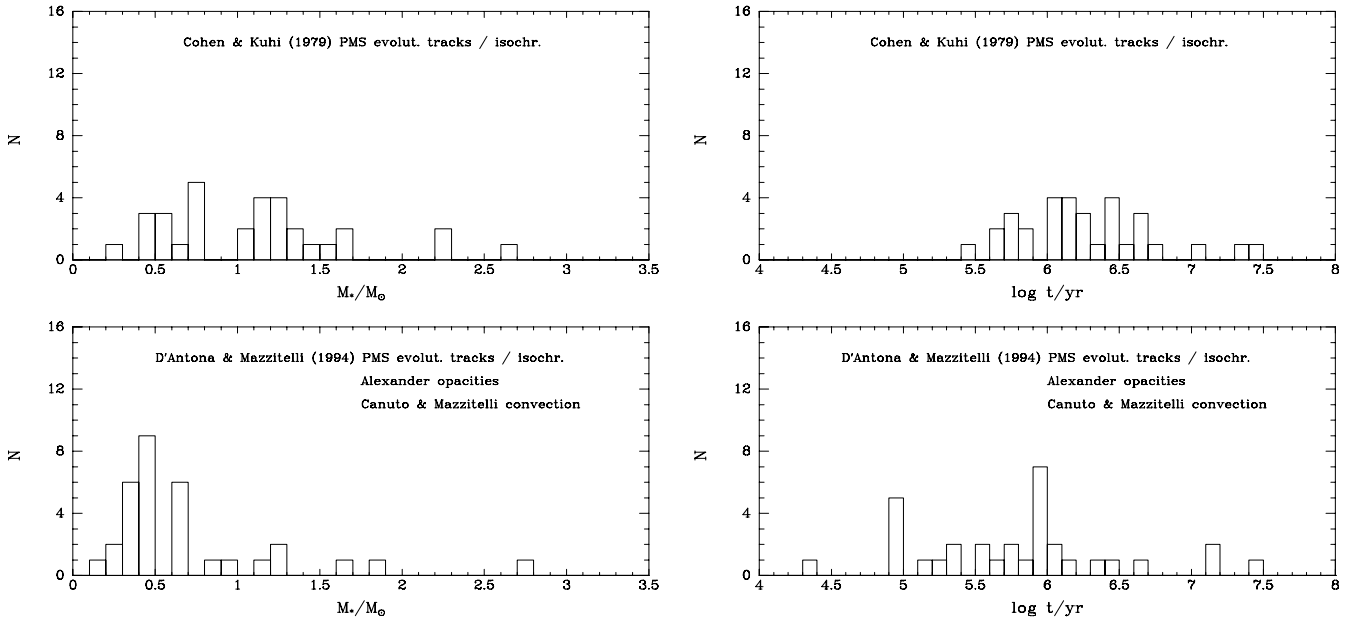

Fig. 2. Distribution of the stellar masses (left) and stellar ages (right) as derived from evolutionary tracks and isochrones by Cohen & Kuhi (1979; top) and D'Antona & Mazzitelli (1994; bottom). Note that six sources are missing in the histograms due to unknown luminosities.

letter behind the ROX number: e.g. ROX 9A, ROX 9B, etc. Bouvier & Appenzeller (1992) obtained low and medium resolution spectrograms, as well as visual and near IR photometry. They derived stellar parameters like spectral type, Hα and Hβ equivalent widths, $T_{\rm eff}$, and L_*. After placing the stars in an H-R diagram they determined stellar masses and ages based on PMS evolutionary tracks and isochrones by Cohen & Kuhi (1979).

For the sake of comparison with a number of recently published 1.3 mm surveys of Hα selected T Tauri stars in Taurus-Auriga (Beckwith et al. 1990, Osterloh & Beckwith 1995), Chamaeleon (Henning et al. 1993), Ophiuchus (André & Montmerle 1994), and Lupus (Nürnberger et al. 1997) we have redetermined the stellar masses and ages using new PMS evolutionary tracks and isochrones provided by D'Antona & Mazzitelli (1994; Fig. 1), which are based on Alexander opacities (Alexander et al. 1989) and Canuto & Mazzitelli convection theory (Canuto & Mazzitelli 1990, 1992). Underlying $\log T_{\rm eff}$ values are recalculated from the spectral type using relations determined by de Jager & Nieuwenhuijzen (1987). Comparing the new mass distribution with the old one, a shift by a factor of two to lower stellar masses is obvious (Fig. 2, left), while we have found no significant effect for the mean value of the stellar ages within the error bars. However, the distribution of stellar ages (Fig. 2, right) derived from the D'Antona & Mazzitelli isochrones is more spread out than the corresponding distribution based on Cohen & Kuhi isochrones.

For six objects (ROX 9A, ROX 9B, ROX 9C, ROX 9D, ROX 14, and ROX 35B) no values for stellar mass and age could be estimated due to unknown luminosities. For the remaining 32 ROX sources stellar ages and masses are given in column 7 and 8 of Table 1. Both the distribution and the mean value of the stellar masses and ages ($\bar{M} \sim 0.7\,M_\odot$, $\bar{t} \sim 6 \cdot 10^5$ yr) are in good agreement with those obtained for T Tauri stars in other star forming regions (see e.g. statistics for Taurus-Auriga and Lupus samples in Nürnberger et al. 1997).

Nevertheless, unknown multiplicity influences the determination of the luminosity and therefore underestimates the stellar age (Simon et al. 1993, Brandner & Zinnecker 1997). Additionally, unresolved multiple sources induce errors in the mass estimates of the individual components, depending on the position in the H-R diagram (Brandner & Zinnecker 1997). Thus, due to uncertain multiplicity and due to neglect of accretion for the PMS tracks, masses and ages of T Tauri stars have a relatively large uncertainty. However, the growing number of extensive surveys for multiple systems in nearby low-mass star forming regions like Chamaeleon, Lupus, Ophiuchus, and Taurus-Auriga (e.g. Mathieu et al. 1989, Reipurth & Zinnecker 1993, Leinert et al. 1993, Simon et al. 1993, 1995, Ghez et al. 1993, 1997, Brandner et al. 1996; see also Sect. 4.3) provides an excellent data base for detailed studies of the physical properties of spatially resolved binary components, e.g. depending on the binary separation or mass ratio.

By comparison with theoretical PMS evolutionary tracks (e.g. from D'Antona & Mazzitelli 1994, Swenson et al. unpublished) Hartigan et al. (1994) and Brandner & Zinnecker (1997) showed that at least 2/3 of the binaries in their samples are coeval. Young binaries turned out to be an important tool for testing PMS evolutionary tracks and isochrones, i.e. for testing the underlying assumptions on the convection model and molecular opacities. Coeval PMS binaries may also provide an important test of circumstellar evolution as a function of component separation and mass ratio (since they are coeval, time does not enter as a variable).

Table 1. Measured and derived parameters for 38 X-ray selected T Tauri stars in Ophiuchus. For a cross identification of the ROX sources with optical counterpart candidates see e.g. Table 2 in Bouvier & Appenzeller (1992).

Name	Sp.T. [1]	EW(Hα)/Å [1]	IR class [2]	log $L_*/L_\odot$ [1]	log T_{eff}/K	log t/yr	$M_*/M_\odot$	$S_{1.3mm}$ (mJy)	σ (mJy)	M_{disk} ($10^{-3}M_\odot$)	M_{disk}/M_* (%)
ROX 2	K3/M0	2.8	III ?	0.7	3.60	(4.3)	0.30	<30*	10	<4.5	<1.5
ROX 3	K3/M0	2.3/2.7 (v)	III ?	-0.2	3.60	6.0	0.48	<30*	10	<4.5	<0.9
ROX 4	K2	2.5		0.7	3.65	5.3	0.70	<28	9	<4.2	<0.6
ROX 5	K7	1.4		-0.2	3.59	5.9	0.42	<19	6	<2.9	<0.7
ROX 6	K6	87/220 (v)	II	0.4	3.60	(4.9)	(0.4)	**31**	6	**4.7**	**1.4**
ROX 7	K7	1.5 (v)	III	-0.2	3.59	5.9	0.42	<20*	7	<3.0	<0.7
ROX 8	K0	-0.6	III	1.5	3.68	(4.9)	1.6	<5*	2	<0.8	<0.1
ROX 9A	M0	-1.0			3.56			<22	7	<3.4	
ROX 9B	K2	-0.5			3.65			<11	4	<1.7	
ROX 9C	K4	-1.0			3.62			<14	5	<2.2	
ROX 9D	G?	-3.8			3.72			<35	12	<5.3	
ROX 10A	K5	20	II	0.2	3.61	5.6	0.44	<25*	8	<3.8	<0.9
ROX 10B$^+$	K0	5	II	1.2	3.68	5.2	1.3	**65**	19	**9.8**	**0.7**
ROX 12	M0	1.2 (v)		-0.7	3.56	6.4	0.40	<19	6	<2.9	<0.7
ROX 14$^+$	B4	-3.5	III		4.25			<15*	5	<2.3	
ROX 16	G9	19	III	0.6	3.69	5.9	1.2	<20*	7	<3.0	<0.3
ROX 20A	M5	3.0	III	-0.3	3.51	(4.9)	0.18	<20*	7	<3.0	<1.7
ROX 20B	M2	6.3	III ?	-0.8	3.53	6.3	0.25	<20*	7	<3.0	<1.2
ROX 21$^+$	K4/M2.5	4.5/8.8 (v)	III	-0.2	3.58	5.8	0.37	<35*	12	<5.3	<1.4
ROX 29	K4/K6	10.5/13.8 (v)	II	0.1	3.61	5.8	0.47	**15***		**2.3**	**0.5**
ROX 30A	G?	-2.0		-0.2	3.72	7.4	0.95	<10	3	<1.5	<0.1
ROX 30B	K4	22.2	II ?	0	3.62	5.9	0.60	<45*	15	<6.8	<1.1
ROX 30C	K4	14.3	II ?	0	3.62	5.9	0.60	**40***		**6.0**	**1.0**
ROX 31$^+$	K7	3.3	III	-0.3	3.59	6.1	0.47	<25*	8	<3.8	<0.8
ROX 33$^+$	G0	21	III	1.3	3.75	6.1	(2.7)	<35*	12	<5.3	<0.2
ROX 34$^+$	M2.5	30/48.3 (v)	II	-0.2	3.53	5.0	0.21	**60***		**9.0**	**4.3**
ROX 35A	K3	-1.0		0.1	3.64	5.9	0.67	<29	10	<4.4	<0.7
ROX 35B	G4	-2.0			3.72			<19	6	<2.8	
ROX 39	K5	3.6/6.0 (v)	III ?	0.3	3.61	5.3	0.42	<30*	10	<4.5	<1.1
ROX 42B$^+$	M0	1.7	III ?	-0.2	3.56	5.7	0.30	<45*	15	<6.8	<2.3
ROX 42C$^+$	K6	1.6 (v)	II	0.4	3.60	(4.9)	(0.4)	<30*	10	<4.5	<1.3
ROX 43A$^+$	G0	1.8/3.4 (v)	II	0.7	3.75	6.6	1.8	<35*	12	<5.3	<0.3
ROX 43B$^+$	K5	0.8		0.2	3.61	5.6	0.44	<17	6	<2.6	<0.6
ROX 44	K3	60.5/76.1 (v)	II	0.3	3.64	5.7	0.61	**105**	11	**15.8**	**2.6**
ROX 45B	K?			-0.6	3.62	7.2	0.83	<19	6	<2.9	<0.4
ROX 45C	K5	-1.0		-0.2	3.61	6.2	0.61	<19	6	<2.9	<0.5
ROX 45D	K0	-1.0		-0.3	3.68	7.2	1.0	<19	6	<2.9	<0.3
ROX 47A	K2/K7-M0	9.2	III	0.2	3.60	5.4	0.37	<20*	7	<3.0	<0.8

Notes: 1.3 mm detections are printed in bold letters, whereas upper limits (3σ) are indicated by a "<". Flux values indicated by * were measured by André & Montmerle (1994) with a single-channel bolometer. Additionally, André & Montmerle (1994) obtained flux values for ROX 6 (70 mJy), ROX 10B (65 mJy), and ROX 44 (110 mJy). For sources with significant time variations of the Hα equivalent width the most extreme observed EW(Hα) values are given followed by a "(v)". The T_{eff} values are calculated from the spectral type using relations determined by de Jager & Nieuwenhuijzen (1987). Stellar masses and ages are based on PMS evolutionary tracks by D'Antona & Mazzitelli (1994). Bracketed values for stellar mass and age are estimated by extrapolation. For our calculations of the disk masses (gas + dust) from the 1.3 mm flux densities, we adopted a mass-averaged dust temperature of 30 K (Nürnberger 1995) and a mass opacity coefficient of 0.02 $cm^2\ g^{-1}$ (Beckwith et al. 1990). A $^+$ behind the source name marks known binaries (Mathieu et al. 1989, Reipurth & Zinnecker 1993, Simon et al. 1995); their separations are given in Table 3.

References: [1] Bouvier & Appenzeller (1992), [2] André & Montmerle (1994).

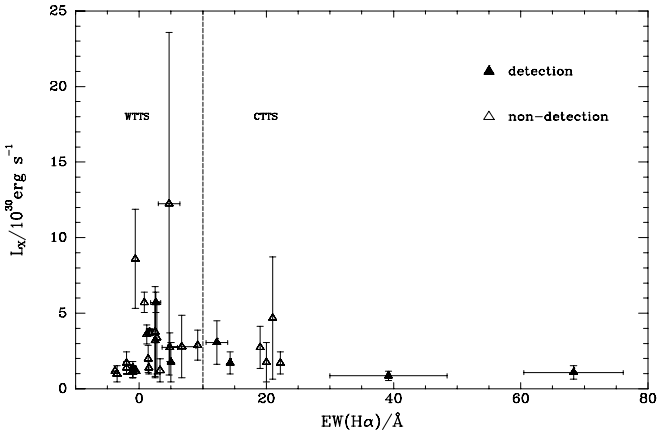

Fig. 3. X-ray luminosity as a function of the equivalent width of the Hα line (EW(Hα) > 0 Å: emission, EW(Hα) < 0 Å: absorption). No clear correlation is seen. The dashed line at EW(Hα) = 10 Å separates WTTS from CTTS. 1.3 mm detections are marked by filled symbols, while sources not detected have 3σ upper limits indicated by open symbols. As the X-ray emission from T Tauri stars is variable due to stellar flares we give mean values for the X-ray luminosity and indicate the range of X-ray variability by error bars. Within the Einstein IPC error circle some X-ray sources have several possible counterparts at optical and IR wavelengths (further explanation is given in Sect. 3). Note that some sources show a variability in EW(Hα), too. ROX 6 is lying outside the plot range.

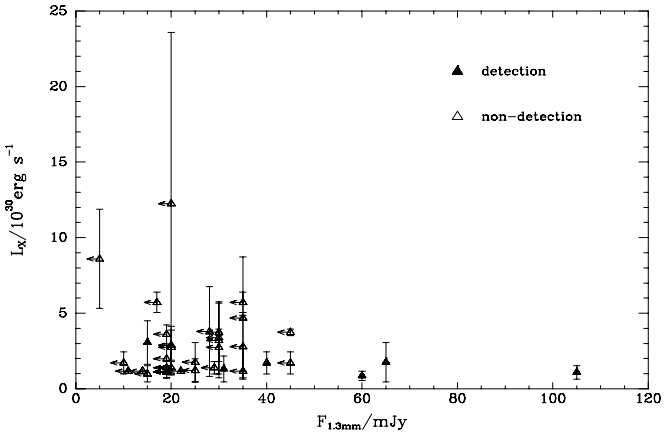

Fig. 4. X-ray luminosity as a function of the 1.3 mm flux density. No clear correlation is seen. For further explanations see Fig. 3.

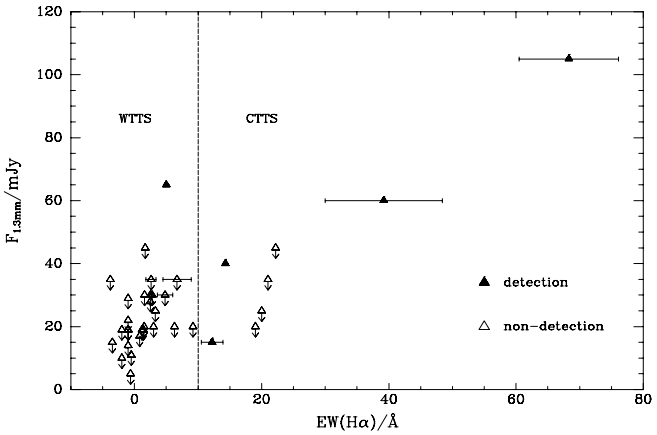

Fig. 5. 1.3 mm flux density as a function of the equivalent width of the Hα line. The correlation probability of 100 % suggests a strong relationship. For further explanations see Fig. 3.

4. Results

In addition to basic stellar parameters which have been discussed already in Sect. 3 we have listed in Table 1 the 1.3 mm flux densities and corresponding statistical uncertainties (column 9 and 10), obtained with the MPIfR 7-channel bolometer array during an observing run at the IRAM 30 m MRT. In order to improve the statistical significance of our conclusions we have combined our own data set (17 ROX sources) with 1.3 mm measurements obtained by André & Montmerle (1994) for 21 ROX sources. Furthermore, several non-parametric tests were performed using the software package ASURV (La Valley et al. 1992). Note, when expressed in terms of an equivalent Gaussian probability, a correlation probability of about 95 % derived from the test models corresponds to a 2σ result.

Because the origin of X-ray emission from T Tauri stars is purely stellar, there is in general no difference in X-ray properties between classical and weak-line T Tauri stars (e.g. Bouvier 1990). Hence it is not surprising, that for our sample of T Tauri stars in Ophiuchus (Fig. 3) there is probably no correlation (correlation probability ~ 70 %) between X-ray luminosity and Hα emission line equivalent width, which is an indicator for the activity in the boundary layer between circumstellar disk and star (see e.g. Bertout et al. 1988).

Similarly, the measured 1.3 mm flux density does not seem to be correlated with the X-ray luminosity (correlation probability ~ 76 %; Fig. 4), which confirms the independence of the X-ray emission from the cold circumstellar environment. Furthermore, there is a strong indication (correlation probability ~ 100 %) for a correlation between the 1.3 mm flux density and the equivalent width of the Hα emission line (Fig. 5), which implies that the Hα emission is probably — but not necessarily (see e.g. André & Montmerle 1994) — related to the amount of circumstellar gas and dust.

4.1. Detection rate

In Table 1 the flux densities of the 1.3 mm detected sources are indicated by bold print, while for non-detections only 3σ upper limits are given for the flux density. An object is considered as detected, if the observed flux density is at least three times (3σ) the measured standard deviation. Owing to a time-variable atmospheric noise, the uncertainty σ was not constant throughout the observing run. Therefore, no uniform lower limit to the flux density could be adopted.

Out of the sample of 38 X-ray selected T Tauri stars, cold dust emission from 6 objects (ROX 6, ROX 10B, ROX 29, ROX 30C, ROX 34, and ROX 44) is detected, corresponding to

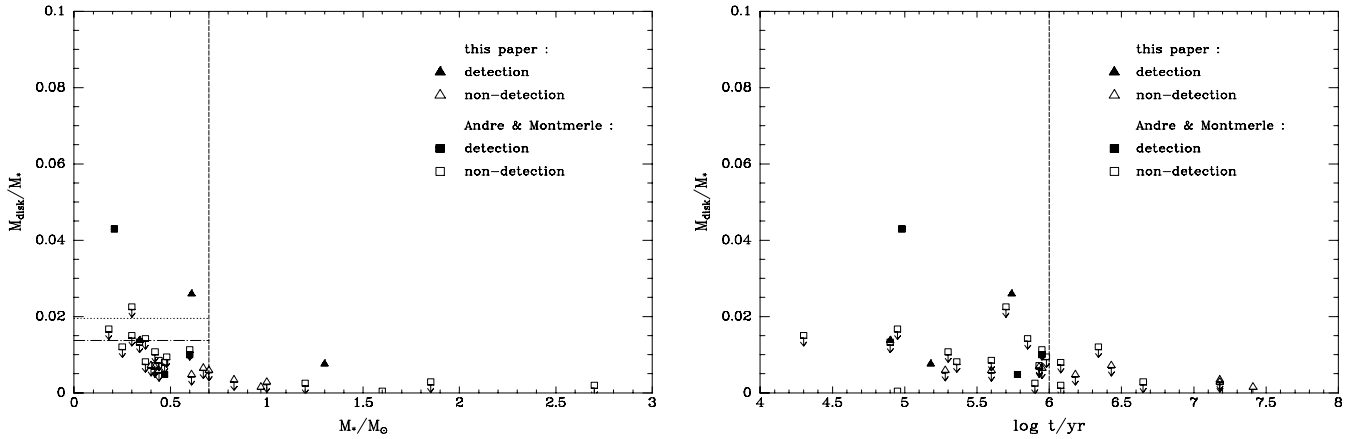

Fig. 6. Ratio of gas + dust mass to stellar mass (relative disk mass) as a function of stellar mass (left) and age (right). Filled symbols indicate detections on the basis of the 3σ detection limit. Open symbols mark 3σ upper limits for non-detections. The dashed line at $M_* = 0.7\,M_\odot$ represents a virtual border-line between T Tauri stars of 'higher mass' and 'lower mass'. The dotted and dash-dotted lines indicate the corresponding mean and median values, both calculated from the 1.3 mm detections only. We obtained no 1.3 mm detection for stars older than 10^6 years, stressed by a dashed line.

Table 2. Correlation probabilities derived from ASURV test models taking upper limits into account.

Correlation test model	Correlation between	
	M_{disk}/M_* and M_*	M_{disk}/M_* and t_*
Cox Prop. Hazard	0.82	0.97
Gen. Kendall's Tau	0.82	0.97
Spearman's Rho	1.00	1.00

Note: When expressed in terms of an equivalent Gaussian probability, a correlation probability of about 95 % derived from the test models corresponds to a 2σ result.

a face value detection rate of 16 %. For the remaining objects 3σ upper limits (~ 21 mJy on average) are derived. Thus, the 1.3 mm detection rate for our sample of X-ray selected T Tauri stars is lower by about a factor of 2 compared to Hα selected T Tauri stars (Beckwith et al. 1990, Osterloh & Beckwith 1995, Henning et al. 1993, André & Montmerle 1994, Nürnberger et al. 1997). This effect can be explained by the relatively large number of WTTS (75 %) in our X-ray selected sample, while Hα selected samples are heavily biased towards CTTS.

Note that — using the MPIfR 7-channel bolometer array — we obtained a 1.3 mm flux for ROX 6 which is smaller by a factor of about 2 than that measured by André & Montmerle (1994) with a single-channel bolometer. In part this might be due to the improved noise reduction which is possible with the bolometer array. Furthermore, the bolometer array allows us to exclude extended dust emission originating from a circumstellar envelope more reliably. Because the discrepancy between the two measurements is significant and presumably not caused by atmospheric effects, it would be interesting to obtain a mm map of this source. We suggest that apart from being an IR class II source ($\alpha_{IR} = -0.7$) ROX 6 possibly possesses a relatively massive circumstellar envelope.

André & Montmerle (1994) have shown in a 1.3 mm continuum survey for cold circumstellar dust in a sample of over 100 YSOs in Ophiuchus that WTTS represent both class II and class III objects (with the majority belonging to the latter class), whereas nearly all CTTS are class II sources. From their studies we have also learned that depending on the stellar evolutionary stage 15 % (IR class III, $t \sim 10^7$ yr), 60 % (IR class II, $t \sim 10^6$ yr), and even up to 80 % (IR class I, $t \sim 10^5$ yr) of the PMS stars with stellar masses in the range $0.1\,M_\odot < M < 2.5\,M_\odot$ are detected at current sensitivities for 1.3 mm continuum emission.

Taking this into account it is obvious that the detection rate found for the ROX sample is in good agreement with the current knowledge of the PMS evolution of T Tauri stars. In other words, the result that all 6 detected sources belong to the IR class II and most of the non-detections are IR class III sources (see Table 1) is well consistent with the evolutionary classification scheme of YSOs, as already mentioned in Sect. 1.

4.2. Circumstellar disk masses

As dusty envelopes / disks around pre-main sequence (PMS) stars are optically thin at wavelengths of the order of 1 mm, the flux density is proportional to the total mass (Beckwith et al. 1986, Sargent & Beckwith 1987). Thus, we have calculated the disk mass (gas + dust) directly from the measured 1.3 mm flux density $S_{1.3mm}$:

$$M_{disk} = M_{gas+dust} = \frac{S_{1.3mm} \cdot d^2}{B(T_{dust}) \cdot \kappa_{1.3mm}} \quad ,$$

where $d \approx 160$ pc is the distance to the Ophiuchus star forming region and $B(T_{dust})$ is the Planck function. We adopted a mass averaged dust temperature of 30 K, which was obtained by fitting Planck functions to the spectral energy distribution

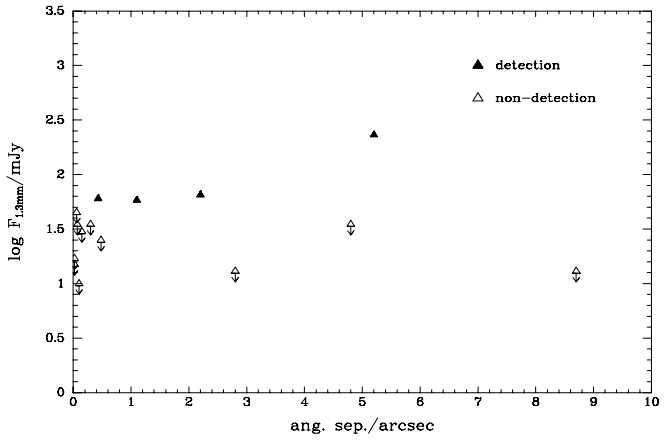

Fig. 7. 1.3 mm flux density as a function of angular separation for 15 binaries in Ophiuchus. The dashed line indicates the 3σ detection limit of the survey. 1.3 mm detections are marked by filled symbols, while non-detections are indicated as 3σ upper limits by open symbols.

at far infrared and mm wavelengths (Nürnberger 1995), ignoring the IRAS 100 μm fluxes due to possible contamination by molecular cloud emission. For the mass opacity coefficient at 1.3 mm we assumed a value of $0.02\,\mathrm{cm^2\,g^{-1}}$ as suggested for circumstellar disks by Beckwith et al. (1990).

The mass of the circumstellar disks is given in column 11 of Table 1. Taking upper limits into account the cold disk masses appear to be less than $5 \cdot 10^{-3}\,\mathrm{M_\odot}$ on average. Both the statistical distribution and the mean value of the disk mass are similar to those obtained for other star forming regions (see e.g. Nürnberger et al. 1997).

In order to gain insight on how cold circumstellar dust masses traced by the 1.3 mm flux density change with stellar mass and age, we have calculated the ratio of circumstellar disk mass to stellar mass, i.e. the relative disk mass (column 12 of Table 1). In Fig. 6 (left) the relative disk mass is plotted as a function of stellar mass (see also the corresponding correlation probabilities in Table 2). In particular, dividing the stellar mass into two bins there seems to be a higher fraction of circumstellar material for $\mathrm{M_*} < 0.7\,\mathrm{M_\odot}$ than for $\mathrm{M_*} > 0.7\,\mathrm{M_\odot}$. Due to the small number of detections in our Ophiuchus sample we have verified and confirmed this effect both in a sample of 32 Hα selected T Tauri stars in Lupus (12 detections) and a sample of 78 Hα selected T Tauri stars in Taurus-Auriga (40 detections; cf. Nürnberger et al. 1997). It might be explained by higher accretion rates for more massive stars (e.g. Yorke 1986, Hillenbrand et al. 1992).

In Fig. 6 (right) we have plotted the relative disk mass as a function of stellar age (again, the corresponding correlation probabilities are given in Table 2). There is no 1.3 mm detection for stars older than 10^6 years, which is slightly earlier in comparison to, but still in agreement with the results found for Hα selected samples in Taurus-Auriga and Lupus ($3 \cdot 10^6 \ldots 10^7$ years; Beckwith et al. 1990, Nürnberger et al. 1997) if typical error bars for $\mathrm{T_{eff}}$ and $\mathrm{L_*}$ (see Fig. 1) are considered. However, although the absolute time at which PMS stars lose their disks is ill-defined and probably also depends on initial conditions (cf. Walter et al. 1988, Montmerle & André 1989, André 1995), this suggests that disks around low mass PMS stars become undetectable at an age of the order $10^6 \ldots 10^7$ years given the sensitivity limit of current ground based mm telescopes. A possible explanation might be found in the reduced amount of small particles: the dust grains either may have coagulated to much greater bodies like planetesimals and protoplanets (e.g. Boss 1996) or may have been dispersed or accreted (Strom et al. 1989).

Table 3. Measured 1.3 mm flux densities and angular separations of 15 PMS binaries in Ophiuchus.

Name	$\mathrm{F_{1.3mm}}$ (mJy)	σ (mJy)	ang. sep. (arcsec)
ROX 10B	**65**	19	2.2
ROX 14	<15*	5	0.02
ROX 21	<35*	12	0.3
ROX 31	<25*	8	0.48
ROX 33	<35*	12	0.07
ROX 34	**60***		0.43
ROX 42B	<45*	15	0.06
ROX 42C	<30*	10	0.15
ROX 43A	<35*	12	4.8
ROX 43B	<17	6	0.02
WSB 4	<13	4	2.8
SR 24	**230**	11	5.2
VSSG 14	<10	3	0.10
EL 2-49	**58**	5	1.1
HBC 652	<13	4	8.7

Notes: 1.3 mm detections are printed in bold letters, whereas upper limits (3σ) are indicated by a "<". Flux values indicated by * were measured by André & Montmerle (1994). The angular separations are measured by Mathieu et al. (1989), Reipurth & Zinnecker (1993), and Simon et al. (1995). SR 24 is a hierarchical triple, as Simon et al. (1995) discovered an IR companion 0.″2 away from SR 24N. The same is true for ROX 34, as component ROX 34A has an IR companion with a separation of 0.″01 (Simon et al. 1995). Also WSB 4 and HBC 652 are expected to be triple systems (Brandner, unpubl.). The binaries ROX 43A and ROX 43B form a quadruple with a separation of 6.″2 between the main components.

4.3. Relationship between 1.3 mm flux and binary separation

In our ROX sample ten sources are known as binaries: ROX 10B, ROX 14, ROX 21, ROX 31, ROX 33, ROX 34, ROX 42B, ROX 42C, ROX 43A, and ROX 43B (Mathieu et al. 1989, Reipurth & Zinnecker 1993, and Simon et al. 1995). Thus, the multiplicity frequency in the separation range 0.″02 to 5.″2 is approximately 26 %, reflecting the results found by Reipurth & Zinnecker (1993; 16 %) for the separation range 1″ to 12″, based on a systematic survey covering 238 objects, and by Leinert et al. (1993; 42 %) for the separation range 0.″13 to 12″, based on their Taurus survey covering 104 young stars. The 1.3 mm flux densities and angular separations of the X-ray selected binaries are listed in Table 3 together with the corresponding values of

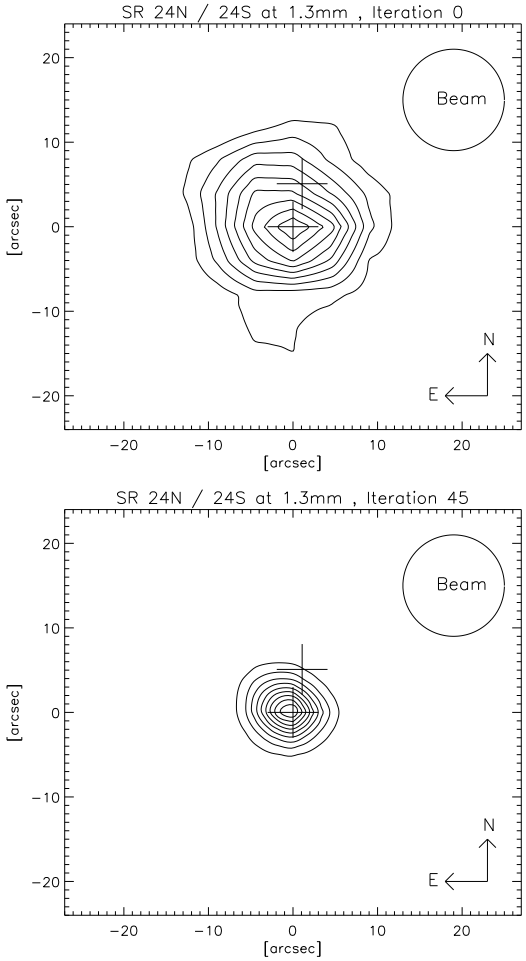

Fig. 8. SR 24N/S mapped at $\lambda = 1.3$ mm with the MPIfR 7-channel bolometer array mounted at the IRAM 30 m MRT. Contour lines correspond to 10, 20, 30, . . ., 90 percent of peak intensity (≈ 230 mJy) before (top) and after (bottom) deconvolution with a Gaussian maximum likelihood algorithm using maps of Uranus and Mars as point spread functions. Crosses mark the positions of the optical counterparts ($V_{\rm SR24N} = 16.0$, $V_{\rm SR24S} = 15.9$, ang. sep. = 5.″2, pos. ang. = 348°).

five additionally observed binaries: WSB 4, SR 24, VSSG 14, EL 2-49, and HBC 652.

Out of this small sample of fifteen binaries in Ophiuchus four are detected at 1.3 mm (indicated by bold print): ROX 10B, ROX 34, SR 24, and EL 2-49. As we have shown in Fig. 7 these 1.3 mm detected binaries have angular separations larger than 0.″4, which — at a distance of 160 pc — corresponds to a projected linear separation of approximately 65 AU. For separations smaller than 0.″4 there were no detections. Even for larger separations four multiple sources (ROX 31, ROX 43A, WSB 4, and HBC 652) are not detected at 1.3 mm. Due to the small number (fifteen binaries) it is not clear whether a (slight) correlation between the 1.3 mm flux density and the binary separation can be inferred. Correlation probabilities range from 70 % to 95 %.

In recent studies Simon et al. (1995), Zinnecker (1995), and Jensen et al. (1996) have investigated the relationship between (sub)mm continuum flux and binary separation for samples of

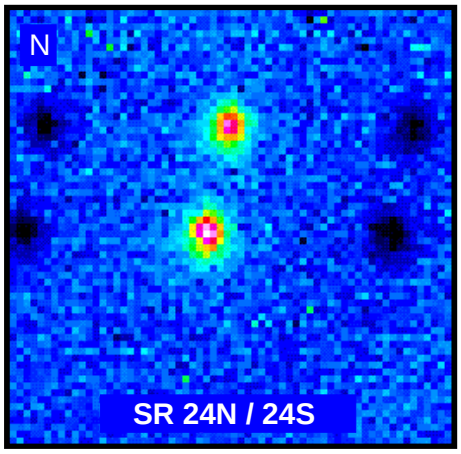

Fig. 9. Mid infrared (N-band) image of SR 24N/S obtained with TIMMI mounted at the ESO 3.6 m telescope on La Silla, Chile (Stanke & Zinnecker 1998). The pixel scaling is 0.″34/pix. Both the northern and the southern component show roughly equal emission ($F_{\rm SR24N} = 1.3$ Jy and $F_{\rm SR24N} = 1.6$ Jy at 10 μm).

PMS binaries in the star forming regions of Ophiuchus, Taurus, and Scorpius. They found that binaries with projected separations in the range of 1 AU to 100 AU have lower submm continuum fluxes than wider binaries or even single stars. This suggests that binaries with separations less than 100 AU significantly influence the nature of their associated disks. Such an interaction between a circumstellar disk and a close companion was already discussed in detail for UZ Tau by Ghez et al. (1994).

4.4. The hierarchical triple SR 24

As a further test case, we have mapped the hierarchical triple SR 24 at $\lambda = 1.3$ mm with the 7-channel bolometer array mounted at the IRAM 30 m MRT (Fig. 8). The separation between the two main components is 5.″2 in the North-South direction. Both SEST 15 m and IRAM 30 m 1.3 mm dust continuum (photometric) measurements centered on the redder, southern component yielded a strong detection (260 mJy, Reipurth et al. 1993; 280 mJy, André & Montmerle 1994; 230 mJy, this paper, Table 3) with a corresponding circumstellar disk mass of $\sim 0.035\,M_\odot$ (gas + dust). Interpreting the map, this cold dust emission is associated with the southern component, while for the northern component we derived an upper limit of 10 % of the SR 24S peak flux density. Due to a possible contamination by the emission of SR 24S, it is not known whether SR 24N is associated with mm emission.

This question has gained in importance, since recent lunar occultation observations have shown that the northern component of SR 24 is itself a close (sub-arcsec) binary system with a separation (0.″2, i.e. ~ 30 AU at the distance of 160 pc; Simon et al. 1995) similar to typical dimensions of circumstellar disks (inner part approximately 1 AU, outer part up to several 100 AU). At $\lambda = 10$ μm, which is an indicator of warm circumstellar dust in the inner part of the disk, both the northern and the southern

component show roughly equal emission (F_{SR24N} = 1.3 Jy and F_{SR24S} = 1.6 Jy at 10 μm; see Fig. 9 as well as Stanke & Zinnecker 1998). Thus, according to the 10 μm measurements the inner part of the disk around SR 24N is still present, while the non-detection of 1.3 mm emission from SR 24N suggests a lack of cold circumstellar dust in the outer part of the disk. This is likely due to enhanced disk accretion/destruction caused by the presence of the close IR companion, as already discussed above (Ghez et al. 1994; Jensen et al. 1996).

In spite of the pointing uncertainty of approximately 3″ at the IRAM 30 m MRT, we note that a circumbinary disk around SR 24 would result in a much more elongated shape of the contour lines.

5. Conclusions

We have presented the results of 1.3 mm dust continuum observations for a sample of 38 X-ray selected T Tauri stars in the Ophiuchus star forming region and compared them with those obtained by 1.3 mm surveys of Hα selected T Tauri stars in several other star forming regions. As our sample of ROX sources is heavily biased towards WTTS, the 1.3 mm detection rate is significantly lower than that typical for Hα selected samples, which mainly consist of CTTS.

From the 1.3 mm flux densities we have estimated the circumstellar disk masses. In agreement with results for T Tauri stars in other star forming regions and independent of the selection criteria we found an average disk mass of less than $5 \cdot 10^{-3}\,M_{\odot}$. Furthermore, there is no 1.3 mm detection for stars older than 10^6 years, which is slightly earlier in comparison to but still consistent with an age of $3 \cdot 10^6 \ldots 10^7$ years found for Hα selected samples. However, although the absolute time at which PMS stars lose their disks is ill-defined and probably also depends on initial conditions, this suggests that at an age of the order $10^6 \ldots 10^7$ years small dust grains in disks around T Tauri stars seem to have coagulated to greater bodies or may have been dispersed or accreted.

For a small sample of 15 multiple sources we made an attempt to investigate the correlation between 1.3 mm dust emission and binary separation. With respect to the 1.3 mm detection of 4 binary systems with projected linear separations larger than 65 AU and the non-detection of all binaries with separations smaller than 65 AU, it seems that the dust continuum emission increases with increasing binary separation. This trend might not be significant, but is in good agreement with results already published by several other authors independently.

Finally, as a further test case for disk destruction scenarios we were able to study in detail the dust distribution of the hierarchical triple system SR 24. Based on the 1.3 mm map we found the dust emission associated with the southern main component of SR 24, while for the northern component we derived only an upper limit of the flux density. At 10 μm both main components show roughly equal emission. These results suggest that SR 24N possesses a more compact disk than SR 24S. As SR 24N has itself a close IR companion a possible explanation might be given by enhanced disk accretion or destruction, which is caused by the presence of the close companion.

Acknowledgements. We thank our anonymous referee for his detailed comments and suggestions, which led to a significant improvement of the manuscript. We also wish to thank Philippe André and Ralf Launhardt for providing us with 1.3 mm maps of Uranus and Mars for deconvolution purposes. Furthermore, we are grateful to Thomas Stanke for releasing the results of the 10 μm photometry of SR 24N/S prior to publication and for many helpful discussions on this specific object. We acknowledge financial support by the Deutsche Forschungsgemeinschaft (DFG) and the Deutsche Agentur für Raumfahrtangelegenheiten (DARA).

References

Adams F.C., Lada C.J., Shu F.H., 1987, ApJ 312, 788
Adams F.C., Lada C.J., Shu F.H., 1988, ApJ 326, 865
Alcalá J.M., Krautter J., Schmitt J.H.M.M., et al., 1995, A&AS 114, 109
Alexander D.R., Augason G.C., Johnson H.R., 1989, ApJ 345, 1014
André P., 1995, in *Circumstellar Dust Disks and Planet Formation*, Proceedings of the 10th IAP Astrophysics Meeting, eds. R. Ferlet, A. Vidal-Madjar, p. 115
André P., Montmerle T., 1994, ApJ 420, 837
Baars J.W.M., Hooghoudt B.G., Mezger P.G., de Jonge M.J., 1987, A&A 175, 319
Beckwith S.V.W., Sargent A.I., Scoville N.Z., et al., 1986, ApJ 309, 755
Beckwith S.V.W., Sargent A.I., Chini R.S., Güsten R., 1990, AJ 99, 924
Bertout C.,Basri G., Bouvier J., 1988, ApJ 330, 350
Blecha A., Richard L., 1989, in *1st ESO / ST-ECF Data Analysis Workshop*, p. 209
Boss A.P., 1996, ApJ 469, 906
Bouvier J., 1990, AJ 99, 946
Bouvier J., Appenzeller I., 1992, A&AS 92, 481
Brandner W., 1992, Diplom thesis, Julius-Maximilians-Universität Würzburg
Brandner W., Zinnecker H., 1997, A&A 321, 220
Brandner W., Alcalá J.M., Kunkel M., Moneti A., Zinnecker H., 1996, A&A 307, 121
Canuto V.M., Mazzitelli I., 1990, ApJ 370, 295
Canuto V.M., Mazzitelli I., 1992, ApJ 389, 724
Casanova S., Montmerle T., Feigelson E.D., André P., 1995, ApJ 439, 752
Cohen M., Kuhi L.V., 1979, ApJS 41, 743
D'Antona F., Mazzitelli I., 1994, ApJS 90, 467
de Jager C., Nieuwenhuijzen H., 1987, A&A 177, 217
Feigelson E.D., Casanova S., Montmerle T., Guibert J., 1993, ApJ 416, 623
Ghez A.M., Neugebauer G., Matthews K., 1993, AJ 106, 2005
Ghez A.M., Emerson J.P., Graham J.R., Meixner M., Skinner C.J., 1994, ApJ 434, 707
Ghez A.M., McCarthy D.W., Patience J.L., Beck T.L., 1997, ApJ 481, 378
Hartigan P., Strom K.M., Strom S.E., 1994, ApJ 427, 961
Henning Th., Pfau W., Zinnecker H., Prusti T, 1993, A&A 276, 129
Hillenbrand L.A., Strom S.E., Vrba F.J., Keene J., 1992, ApJ 397, 613
Jensen E.L.N., Mathieu R.D., Fuller G.A., 1996, ApJ 458, 312

Kreysa E., 1992, in *Photon Detectors for Space Instrumentation*, ESA SP-356, p. 207
Lada C.J., 1987, in *Star Forming Regions*, IAU Symp. No. 115, eds. M. Peimbert, J. Jugaku, p. 1
LaValley M., Isobe T., Feigelson E.D., 1992, in *Astronomical Data Analysis Software and Systems I*, ASP Conference Series Vol. 25, eds. D.M. Worrall, C. Biemesderfer, J. Barnes, p. 245
Leinert Ch., Zinnecker H., Weitzel N., et al., 1993, A&A 278, 129
Mathieu R.D., Walter F.M., Myers P.C., 1989, AJ 98, 987
Meinel E.S., 1986, J. Opt. Soc. Am. 3, 52
Mezger P.G., Sievers A., Zylka R., et al., 1992, A&A 265, 743
Montmerle T., André P., 1989, in *Low Mass Star Formation and Pre-Main Sequence Objects*, ESO Conference and Workshop Proceeding No. 33, ed. B. Reipurth, p. 407
Montmerle T., Casanova S., 1995, RevMexAA (Serie de Conferencias) 1, 329
Montmerle T., Koch-Miramond L., Falgarone E., Grindlay J.E., 1983, ApJ 269, 182
Montmerle T., André P., Casanova S., Feigelson E.D., 1994, in *Cosmical Magnetism*, ed. D. Lynden-Bell, p. 33
Neuhäuser R., Sterzik M.F., Schmitt J.H.M.M., Wichmann R., Krautter J., 1995, A&A 297, 391
Nürnberger D., 1995, Diplom thesis, Julius-Maximilians-Universität Würzburg
Nürnberger D., Chini R., Zinnecker H., 1997, A&A 324, 1036
Osterloh M., Beckwith S.V.W., 1995, ApJ 439, 288
Preibisch Th., Zinnecker H., Schmitt J.H.M.M., 1993, A&A 279, L33
Reipurth B., Zinnecker H., 1993, A&A 278, 81
Reipurth B., Chini R., Krügel E., Kreysa E., Sievers A., 1993, A&A 273, 221
Sargent A.I., Beckwith S.V.W., 1987, ApJ 323, 294
Simon M., Ghez A.M., Leinert Ch., 1993, ApJ 408, L33
Simon M., Ghez A.M., Leinert Ch., et al., 1995, ApJ 443, 625
Sonnhalter C., Preibisch Th., Yorke H.W., 1995, A&A 299, 545
Stanke Th., Zinnecker H., 1998, A&A, submitted
Sterzik M.F., Alcalá J.M., Neuhäuser R., Schmitt J.H.M.M., 1995, A&A 297, 418
Strom K.M., Strom S.E., Edwards S., Cabrit S., Skrutskie M.F., 1989, AJ 97, 1451
Terebey S., Chandler C.J., André P., 1993, ApJ 414, 759
Thum C., Kreysa E., John D., et al., 1992, IRAM Working Report 212
Walker C.K., Carlstrom J.E., Bieging J.H., 1993, ApJ 402, 655
Walter F.M., Brown A., Mathieu R.D., Myers P.C., Vrba F.J., 1988, AJ 96, 297
Wichmann R., Krautter J., Schmitt J.H.M.M., et al., 1996, A&A 312, 439
Wichmann R., Krautter J., Covino E., et al., 1997, A&A 320, 185
Wilking B.A., Schwartz R.D., Blackwell J.H., 1987, AJ 94, 106
Wilking B.A., Lada C.J., Young E.T., 1989, ApJ 340, 823
Yorke H.W., 1986, ARA&A 24, 49
Yorke H.W., Bodenheimer P., Laughlin G., 1995, ApJ 443, 199
Zinnecker H., 1995, in *Circumstellar Dust Disks and Planet Formation*, eds. R. Ferlet, A. Vidal-Madjar, p. 155

This article was processed by the author using Springer-Verlag LaTeX A&A style file *L-AA* version 3.